Available online at www.sciencedirect.com
ScienceDirect
ELSEVIER
Ceramics International 35 (2009) 2145–2149
CERAMICS INTERNATIONAL
www.elsevier.com/locate/ceramint

Simultaneous synthesis and densification of α-Zr(N)/ZrB_2 composites by self-propagating high-temperature combustion under high nitrogen pressure

Shingo Nakane[a,*], Takaya Endo[b], Ken Hirota[b]

[a] *Nippon Electric Glass Co., Ltd., Seiran 2-7-1, Otsu, Shiga 520-8639, Japan*
[b] *Faculty of Engineering, Doshisha University, Kyo-tanabe, Kyoto 610-0321, Japan*

Received 3 October 2008; received in revised form 10 October 2008; accepted 24 November 2008
Available online 13 January 2009

Abstract

Simultaneous synthesis and densification of α-Zr(N)/ZrB_2 composites from a 85 mol% Zr/15 mol% B mixed-powder compacts have been achieved by self-propagating high-temperature under a nitrogen pressure of 10 MPa. Composites consist of fine and short rodlike ZrB_2 grains (0.1 μm^{ϕ}–0.5 μm^{l}) dispersed into α-Zr(N) matrix (3 μm). Dense composite materials (96.5% of theoretical) exhibit excellent mechanical properties, in which their bending strength and H_v are 560 MPa and 6.5 GPa, respectively. This bending strength is much superior to those (205 and 480 MPa) of dense equi-axial α-Zr(N) (10 μm) and dense ZrB_2 (6 μm). Fine and rodlike ZrB_2 grains greatly enhanced their mechanical properties.

Keywords: B. Composites; C. Mechanical properties; D. Borides

1. Introduction

Self-propagating high-temperature combustion synthesis (SHS) is an interesting process in which inorganic initial reactants, just after ignition, transform instantaneously into products with a high exothermic heat originated from their high formation enthalpies [1–3]. As usually SHS products are coarse powders or porous materials, however, a fabrication of dense bulk materials using SHS under high-pressure reacting gas (nitrogen) has been reported by the present authors [4–6]. When SHS reactions occur in a pressurized nitrogen, the gas is believed to (i) act as an elemental source for nitride ceramics, (ii) generate sufficient heat for producing molten phase in gas–solid reaction, (iii) absorb residual gas remaining in isolated pores into product, and (iv) assist isostatic pressing of the molten product.

The new simultaneous synthesis and densification technique was applied to simple Zr–N system [4]. Hexagonal α-Zr(N) solid solution materials technique showed high relative densities from 85.5 to 99.0%, depending on both Zr-powder compacting pressure (50–350 MPa) and SHS-nitrogen pressure (4–10 MPa). Their homogeneous microstructures were composed of fine grains (12–4.5 μm) containing nitrogen of 12.2–23.5 at%, respectively. Mechanical properties of the most highly sintered α-Zr(N) materials ($ZrN_{0.22}$) were evaluated; three-point bending strength σ_b and Vickers hardness H_v were 205 MPa and 6.2 GPa, respectively. Although the σ_b value was almost the same as that (∼205 MPa) of ZrN_{1-x} ($x = 0.047$, cubic structure) [7] and the H_v was much improved in comparison with that (1.4 GPa) of pure metal Zr [8], the strength is not enough to use as structural materials.

In the present study, the SHS technique was applied to the Zr–B–N system, expecting that an addition of B to Zr–N system would allow to form borides in α-Zr(N) and the borides could improve the hardness and the bending strength [9]. This paper deals with the simultaneous synthesis and densification of ZrB_2/α-Zr(N) with easy preparation of the SHS technique.

2. Experimental procedure

As-received metal Zr powder (99.9% pure, average particle size of 12 μm; Kojundo Chemical Co. Ltd., Saitama, Japan) and amorphous B powder (99.9% pure, average particle size of 0.5 μm; Nippon New Metal Co. Ltd., Osaka, Japan) were used as starting materials. An appropriate amount of both powders was mixed in ethanol for 60 min using an alumina mortar and pestle. The mixed powders with various compositions as shown

---

* Corresponding author. Tel.: +81 77 583 9718; fax: +81 77 534 3572.
E-mail address: snakane@neg.co.jp (S. Nakane).

0272-8842/$34.00
doi:10.1016/j.ceramint.2008.11.024

Table 1
Green and relative densities of mixed-powder compacts with various Zr/B atomic ratios.

Samples	Zr/B ratio (at%)	Green density (Mg m^{-3})	Theoretical density (Mg m^{-3})	Relative density (%)
(1)	100/0	4.54	6.50	69.8
(2)	95/5	4.56	6.39	71.4
(3)	90/10	4.63	6.28	73.7
(4)	85/15	4.61	6.15	75.0
(5)	80/20	4.53	6.02	75.2
(6)	70/30	4.36	5.74	75.9

in Table 1 were uniaxially pressed into cylindrical compacts (20 mm in diameter and ~10 mm in height) at 10 MPa and isostatically cold-pressed at 200 MPa. Their green and relative densities, the latter of which were calculated using the theoretical densities of Zr (6.50 Mg m^{-3}) [10] and amorphous B (1.73 Mg m^{-3}) [11], are also shown in Table 1. The relative densities increased from 69.8 to 75.9% with increasing B content. This is due to the fine B particles which fulfill into the cleavages between large Zr particles under an isostatic high pressure of 200 MPa.

The green compacts were put into a carbon crucible, then it was placed in a stainless-steel high-pressure chamber. After evacuation, nitrogen gas (99.99% pure) was introduced into the chamber, and then the compacts were ignited by a carbon ribbon heater which was applied by an electric voltage of ~45 V and a current of ~25 A. Self-propagating high-temperature synthesis was performed under a nitrogen pressure of 10 MPa. The combustion temperature was measured at center position of the sample through a silica glass window with a two-color pyrometer. The combustion temperature reached >3000 °C which is much higher than the melting points of Zr (1855 °C) and B (2092 °C) [12].

SHS products were examined by X-ray diffraction (XRD: Rint 2500, Rigaku, Osaka, Japan) using Cu Kα_1 radiation equipped with a graphite monochromator under a goniometer scanning speed of 0.25° min^{-1}. Scanning electron microscopy (SEM) was utilized for microstructural observations. After phase identification, test bars (~3 mm × 4 mm × 18 mm) for the measurement of mechanical properties were cut from the sintered compacts with a diamond saw and then lapped with a diamond paste (a nominal size of 1–3 μm). Three-point bending strength (σ_b) was measured with a span length of 12 mm and a cross-head speed of 0.5 mm min^{-1}. Vickers hardness (H_v) was determined using the microindentation technique with a load of 49.0 N. Each data point represents the average of 4–6 samples.

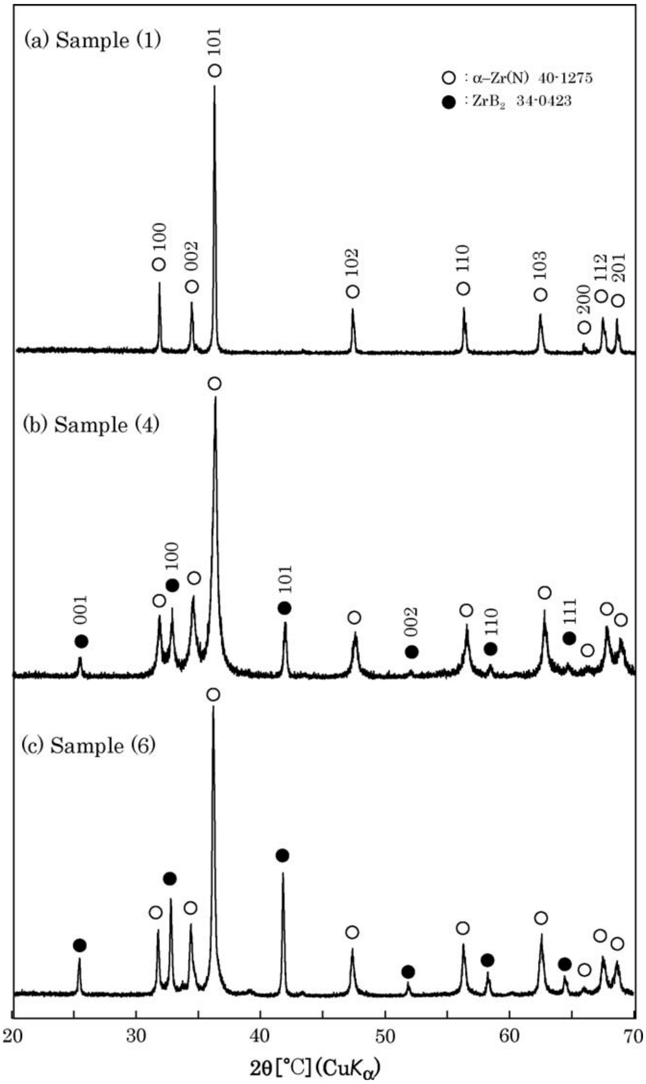

Fig. 1. X-ray diffraction patterns of the products obtained by SHS. (a) Sample 1, (b) sample 4, and (c) sample 6.

3. Results and discussion

3.1. SHS products

Dense bulk materials were obtained as the combustion products. The XRD patterns of the SHS products of (1) (Zr/B = 100/0 at%), (4) (85/15), and (6) (70/30) are shown in Fig. 1(a)–(c); α-Zr(N) and ZrB$_2$ were synthesized [13,14], and

Table 2
Characteristics of the SHS products obtained under a nitrogen pressure.

Sample	Zr/B ratio (at%)	Ratio (at%)	N content (at%)		x of ZrN$_x$	Theoretical density (Mg m^{-3})	Bulk and relative densities (Mg m^{-3}, %)
			(ICP)	(EMGA)			
(1)	100/0	100/0	21	23	0.30	6.81	6.54 (96.0)
(2)	95/5	97/3	–	18	0.24	6.71	6.42 (95.7)
(3)	90/10	94/6	–	14	0.19	6.64	6.36 (95.8)
(4)	85/15	91/9	12	11	0.15	6.60	6.35 (96.2)
(5)	80/20	88/12	–	9	0.12	6.55	6.23 (95.1)
(6)	70/30	79/21	5	5	0.10	6.50	6.10 (93.8)

no other peaks were detected in all samples. Interplanar spacings of ZrB_2 were measured with the aid of an internal standard of high-purity silicon, and unit-cell values were determined by a least-squares refinement. The lattice parameters were $a = 3.166$ nm and $c = 3.528$ nm, agreeing with data ($a = 3.169$ nm, $c = 3.530$ nm) reported previously [14].

Nitrogen content in the product as α-Zr(N) was measured by spectrochemical analysis, *i.e.*, non-dispersive infrared absorption spectrum using inert gas fusion in an impulse furnace (EMGA/620W, Horiba, Kyoto, Japan); in addition to this, induced coupled plasma (ICP: ICAP-55, Thermoelectron Japan, Yokohama, Japan) analysis was also used to determine the nitrogen content. Table 2 shows the nitrogen contents and the chemical formula of α-Zr(N). The nitrogen contents decreased monotonously with increasing B content. This might be due to increase in relative density of starting powder compact resulting in decrease in quantity of nitrogen gas into the compact when SHS reaction.

After the composite materials were polished with a diamond paste, the bulk densities were measured by the Archimedes method. The relative densities were estimated using the theoretical densities of ZrB_2 (6.10 Mg m^{-3}) [14] and α-Zr(N) calculated from the molecular weight, $Z = 2$ [13], Avogadro's number, and lattice parameters thus obtained. The relative densities of all samples are almost 95–96%. Thus, it was formed that dense composite materials were successfully fabricated directly from Zr/B mixed powders by SHS under high nitrogen pressure.

3.2. Microstructure of the products

As shown in Fig. 2(a)–(c), samples (1) and (4) contained only small pores distributed homogeneously. However large pores were observed in sample (6) which contained the largest quantities of ZrB_2. The large pores were formed in the melt in the SHS reaction because the shape of the pores was almost round. It is speculated that the existence of a large amount of ZrB_2 may increase the viscosity of the melt during SHS process, which will suppress the densification.

Fig. 3 shows a SEM photograph for the fracture surface of sample (4), indicating that a morphology of ZrB_2 grains was short rodlike; the average size of these was 0.1 μm wide and 0.5 μm length. Our preliminary experiment indicates monolithic ZrB_2 ceramics consist of granular grains and no rodlike grains are observed (Fig. 4), where ZrB_2 powder was sintered at 1700 °C and 30 MPa using a spark plasma sintering. The noticeable difference is considered to be due to formation of ZrB_2 from the melt in the SHS process where the new formed ZrB_2 can grow freely. In SHS studies on Ti–B system [5], similar rodlike morphology of TiB is also observed in their products in which the combustion temperature is much higher than the melting points of raw materials.

(a) Sample (1)

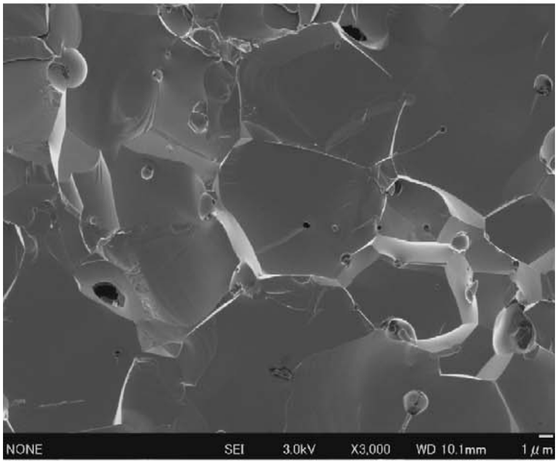

(b) Sample (4)

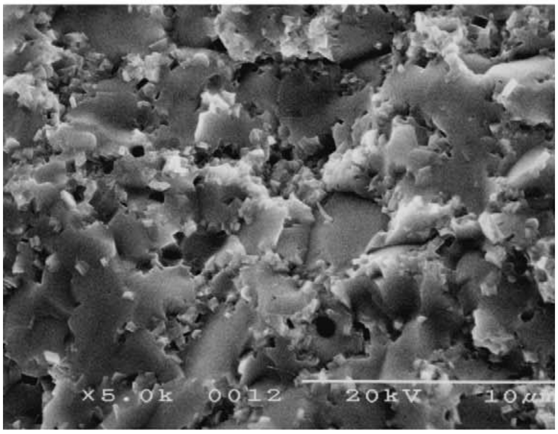

(c) Sample (6)

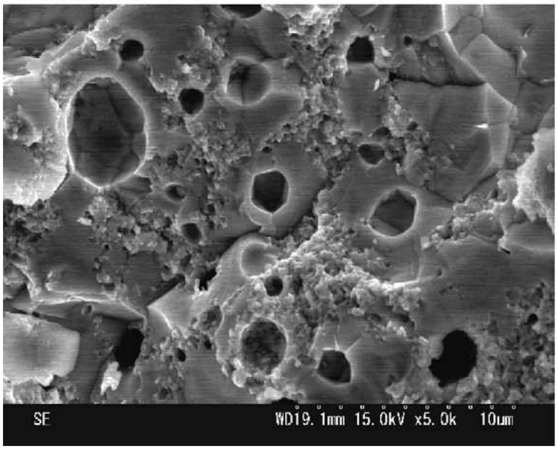

Fig. 2. SEM photographs for fracture surface of the products. (a) Sample 1, (b) sample 4, and (c) sample 6.

Moreover, it should be noted that ZrB_2 and α-Zr(N) grains were smaller in size than the starting Zr powder particles (12 μm). Nucleation and nuclear growth play an important role in the microstructural development of polycrystalline particles during a consolidation from the melt. It can be considered that small grains, corresponding to the nucleation step, were produced by rapid quenching from the molten state. As will be described, the fine and unique microstructure resulted in the improvement of the bending strength.

3.3. Mechanical properties of the products

Fig. 5 shows the values of (a) σ_b and (b) H_v of the SHS products as a function of ZrB_2 content. Strength increased from

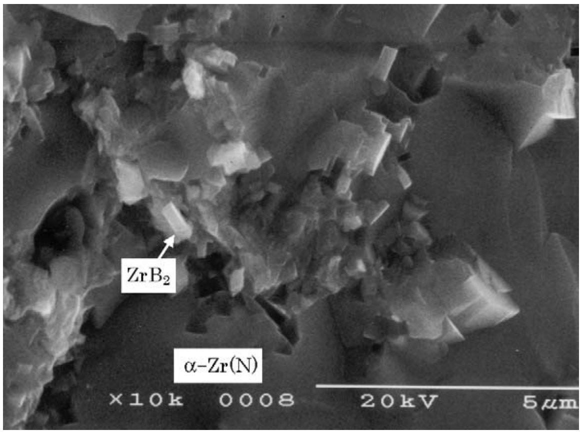

Fig. 3. SEM photograph for fracture surface of the product fabricated by SHS from 85 at% Zr/15 at% B under a high nitrogen pressure.

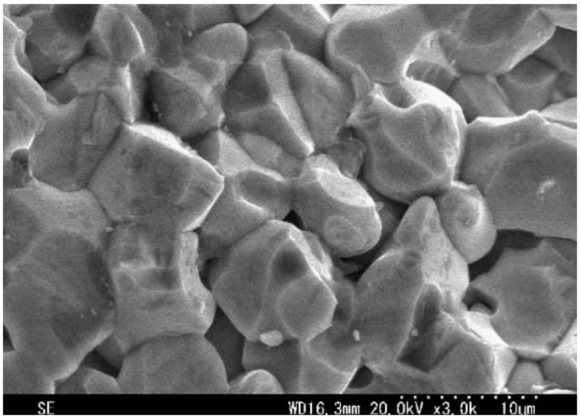

Fig. 4. SEM photograph for fracture surface of monolithic ZrB$_2$ ceramics sintered by SPS (1700 °C/30 min/30 MPa).

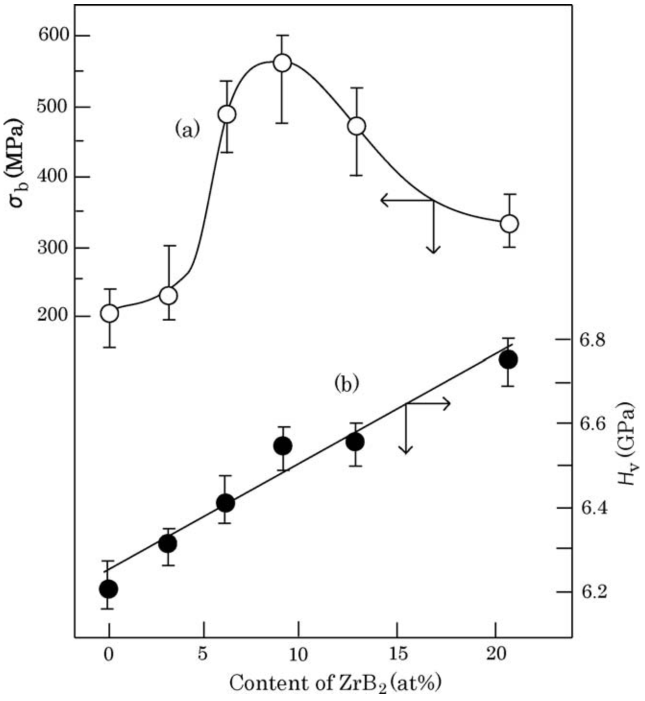

Fig. 5. Mechanical properties of α-Zr(N)/ZrB$_2$ materials fabricated from mixed Zr and B powders under nitrogen pressure.

200 to 560 MPa and then decreased to 320 MPa with increasing ZrB$_2$ content. Fracture toughness (K_{IC}) of sample (4) containing 9 at% ZrB$_2$ is 5.7 MPa m$^{1/2}$. The bending strength of sintered pure ZrB$_2$ and α-Zr(N) reported previously were as follows: the former (σ_b = 480 MPa, G_s = 6 μm, 99% of relative density) [15] and the latter (σ_b = 205 MPa, G_s = 10 μm, 99% of relative density) [4]. These results indicate that the bending strength of the composite materials was much superior to that of the monolithic material of ZrB$_2$. It was reported that a decrease in grain size of ceramics improved their bending strength [16], and it is well-known that elongated grains often enhance the strength of inorganic polycrystalline materials [17]. Therefore, the improved bending strength of the composite materials may be explained in terms of the presence of the fine and short rodlike ZrB$_2$ grains. However, further addition of B than sample (4), the bending strength decreased because of the presence of large pores as shown in Fig. 2(c).

Vickers hardness (H_v) increased linearly from 6.2 to 6.8 GPa with increasing ZrB$_2$ content as shown in Fig. 5(b). This will be due to an increase of ZrB$_2$ content, H_v of which (14.5 GPa)^{20} is much higher than that (6.2 GPa) [4] of α-Zr(N).

4. Conclusions

Self-propagating high-temperature synthesis (SHS) usually has produced various kinds of coarse powders or porous materials. In the present study, dense α-Zr(N)/ZrB$_2$ composite bulk materials have been fabricated by this method under a reacting N$_2$ gas of 10 MPa. α-Zr(N)/ZrB$_2$ = 9/91 mol% material exhibits higher three-point bending strength σ_b of 560 MPa than those of ZrB$_2$ and α-Zr(N) materials. Improved mechanical properties of the composite materials may be explained in terms of the presence of fine and rodlike ZrB$_2$ grain (0.1 μm^{Φ}–0.5 μm^{l}) dispersed into the α-Zr(N) matrix (3 μm).

References

[1] A.G. Merzhanov, I.P. Borovinskaya, Self-propagating high-temperature synthesis of refractory inorganic compounds, Dokl. Acad. Nauk SSSR 204 (2) (1972) 366–369.

[2] Z.A. Munir, Synthesis of high temperature materials by self-propagating combustion methods, Am. Ceram. Soc. Bull. 67 (2) (1988) 342–349.

[3] J. Subrahmanyam, M. Vijayakumar, Review self-propagating high-temperature synthesis, J. Mater. Sci. 27 (23) (1992) 6249–6273.

[4] O. Yamada, Y. Miyamoto, K. Hirota, S. Nakane, M. Yoshinaka, O. Yamaguchi, Simultaneous synthesis and densification of α-Zr(N) by self-propagating combustion under nitrogen pressure, Int. J. Soc. Mater. Eng. Resour. 7 (1) (1999) 188–194.

[5] S. Nakane, O. Yamada, Y. Miyamoto, M. Yoshinaka, K. Hirota, O. Yamaguchi, Simultaneous synthesis and densification of TiB/α-Ti(N) composite material by self-propagating combustion under nitrogen pressure, Solid State Commun. 110 (1999) 447–450.

[6] O. Yamada, M. Hachiya, S. Nakane, M. Yoshinaka, K. Hirota, O. Yamaguchi, Simultaneous synthesis and densification of α-Ti(N) by self-propagating high-temperature combustion under nitrogen pressure, J. Mater. Sci. Lett. 18 (1999) 363–365.

[7] K. Endo, New Handbook of High-Temperature Compounds, Nisso Tsushinsha, Wakayama, Japan, 1994.

[8] T.R.G. Kutty, K. Ravi, C. Ganguly, Studies on hot hardness of Zr and its alloys for nuclear reactors, J. Nucl. Mater. 265 (1999) 91–99.

[9] D.R. Linde, Handbook of Chemistry and Physics, 75th ed., CRC Press, London, 1994.

[10] X-ray Powder Data File, Card no. 5-0665, Joint Committee on Powder Diffraction Standard, Swarthmore, PA, 1960.

[11] Boron, Dictionary for Physics and Chemistry, 3, Iwanami Shoten, Tokyo, 1981.

[12] A.E. McHale, Phase Equilibria Diagrams, vol. X, The American Ceramic Society, Ohio, 1994.

[13] X-ray Powder Data File, Card no. 40-1275, Joint Committee on Powder Diffraction Standard, Swarthmore, PA, 1960.

[14] X-ray Powder Data File, Card no. 34-0423, Joint Committee on Powder Diffraction Standard, Swarthmore, PA, 1960.

[15] A.L. Chamberlain, W.G. Fahrenholtz, G.E. Hilmas, D.T. Ellerby, High-strength zirconium diboride-based ceramics, J. Am. Ceram. Soc. 87 (6) (2004) 1170–1172.

[16] M.N. Rahman, Ceramic Processing of Sintering, Marcel Dekker, New York, Mater. Eng. 10 (1995).

[17] F.F. Lange, Relation between strength, fracture energy, and microstructure of hot pressed Si_3N_4, J. Am. Ceram. Soc. 56 (1973) 518–522.